Shape of the zeroth Landau level in graphene with nondiagonal disorder

Rajesh K. Malla and M. E. Raikh
Department of Physics and Astronomy, University of Utah, Salt Lake City, Utah 84112, USA

(Received 26 November 2018; published 11 February 2019)

Nondiagonal (bond) disorder in graphene broadens Landau levels (LLs) in the same way as random potential. The exception is the zeroth LL, $n = 0$, which is robust to the bond disorder, since it does not mix different $n = 0$ states within a given valley. The mechanism of broadening of the $n = 0$ LL is the intervalley scattering. Several numerical simulations of graphene with bond disorder had established that $n = 0$ LL is not only anomalously narrow but also that its shape is very peculiar with three maxima, one at zero energy, $E = 0$, and two others at finite energies $\pm E$. We study theoretically the structure of the states in $n = 0$ LL in the presence of bond disorder. Adopting the assumption that the bond disorder is strongly anisotropic, namely, that one type of bonds is perturbed much stronger than other two, allowed us to get an analytic expression for the density of states which agrees with numerical simulations remarkably well. On the qualitative level, our key finding is that delocalization of the $E = 0$ state has a dramatic back effect on the density of states near $E = 0$. The origin of this unusual behavior is the strong correlation of eigenstates in different valleys.

DOI: 10.1103/PhysRevB.99.085415

I. INTRODUCTION

Broadening of the Landau levels (LLs) in two-dimensional (2D) electron gas by a random potential was studied more than a quarter century ago in various limits, namely, strong and weak magnetic field, and also short-range and long-range disorder [1–12].

With regard to LLs in graphene [13,14] the theories of the LL broadening of Refs. [1–12] apply. Recent experimental and theoretical studies of the LLs in graphene in the presence of disorder are reported in Refs. [15–19].

There is, however, a situation when the underlying mechanism of the LL broadening in graphene is distinctively different from that in the 2D gas. The tight-binding Hamiltonian of the disordered graphene in magnetic field has the form

$$\hat{H} = \sum_i V_i c_i^\dagger c_i + \sum_{\langle i,j\rangle} (t_{i,j} e^{i\theta_{i,j}} c_i^\dagger c_j + \text{H.c.}), \tag{1}$$

where the $\langle i, j\rangle$ correspond to neighboring sites and the sum runs over all the sites. The Peierls phase $\theta_{i,j}$ is defined in such a way that the sum of the phases around a unit cell is equal to the magnetic flux (in the units of flux quantum) threading the cell. It follows from Eq. (1) that the disorder can be of two types: randomness in on-site energies, V_i, describes the potential disorder, while the randomness in the hopping integrals $t_{i,j}$ describes the bond disorder specific for graphene. To describe the LL broadening due to V_i, one can use the continuous version of the bare Hamiltonian Eq. (1),

$$\hat{H}_0 = V(\boldsymbol{r}) \cdot I + v_F \boldsymbol{\pi} \cdot \boldsymbol{\sigma}, \tag{2}$$

where $\boldsymbol{\sigma}$ is the 2D vector whose projections are the Pauli matrices, and v_F is the Fermi velocity. The effective momentum operator is given by $\boldsymbol{\pi} = \boldsymbol{p} - e\boldsymbol{A}/c$, with $\boldsymbol{p}$ being the electron momentum, and $\boldsymbol{A} = (0, Bx)$ is the vector potential with B standing for the uniform magnetic field.

To make a connection to Refs. [1–12], the Fourier component $V_{\boldsymbol{q}}$ of the random potential $V(\boldsymbol{r})$ is expressed through the random energies V_i used in numerical simulations, as $\sum_i V_i \exp(i\boldsymbol{q} \cdot \boldsymbol{r}_i)$.

Unlike the potential disorder, the bond disorder corresponds to the randomness in v_F and B and, thus, is called nondiagonal disorder. Indeed, v_F is related to the average $\langle t_{i,j}\rangle = t$ as $v_F = \frac{\sqrt{3}ta}{2\hbar}$, where a is the lattice constant. In this way, the fluctuations of $t_{i,j}$ translate into the position-dependent v_F. Similarly, the fluctuations of $\theta_{i,j}$ translate into the position-dependent magnetic field.

The broadening of LLs in graphene due to nondiagonal disorder has been studied numerically in Refs. [20–27]. The results of simulations in all the above papers are consistent with each other. The most prominent feature of these results is that the broadening of $n \neq 0$ levels is much stronger than the broadening of the $n = 0$ level. This feature can be easily understood from the continuous Hamiltonian Eq. (2). Indeed, the eigenfunctions of $\hat{H}_0$ are the spinors

$$\Psi_{n,k}(x, y) = \frac{C_n}{\sqrt{L}} \exp(iky) \begin{pmatrix} \text{sgn}(n)(-i)\phi_{|n|-1,k} \\ \phi_{n,k} \end{pmatrix}, \tag{3}$$

where L is the normalization length. The constant C_n is equal to $1/2$ for $n \neq 0$, and $C_0 = 1$. The functions $\phi_{n,k}(x)$ are the eigenfunctions of the harmonic oscillator

$$\phi_{n,k}(x) = (2^n n! \sqrt{\pi}\ell_B)^{-1/2} e^{-(x-k\ell_B^2)^2/2\ell_B^2} H_n\left[\left(x - k\ell_B^2\right)/\ell_B\right], \tag{4}$$

where $H_n(x)$ is the Hermite polynomial and $\ell_B = (\frac{\hbar c}{eB})^{1/2}$ is the magnetic length. The difference between $n = 0$ LL and other LLs is that the matrix element of nondiagonal disorder between the states k and k' is zero for $n = 0$. This is because one of the two components of the spinor Eq. (3) is zero. In fact, this matrix element remains zero even when the admixtures of

higher LLs to $n = 0$ LL are taken into account, which is the manifestation of the Atiyah-Singer theorem [28]. Therefore, the broadening of $n = 0$ LL is absent in the continuous limit. Finite broadening requires virtual transitions with large momentum transfer. This explains why the width of $n = 0$ LL in the simulations of Refs. [24,26] dropped off dramatically with increasing the correlation radius of $t_{i,j}$.

In all the simulations [20–27] the shape of the broadened $n = 0$ LL was very nontrivial. It differed from conventional Gaussian in two respects: (i) it exhibited a shallow *minimum* at the center and (ii) it possessed a very narrow peak *on top of this minimum*. Neither analytical description nor even theoretical interpretation of this peculiar shape are available. The goal of the present paper is to provide such an interpretation. In addition to the broadening, the authors of Refs. [20–27] studied the localization properties of the $n = 0$ eigenstates with nondiagonal disorder. It was established that there are *two* split delocalized states away from the center. In Ref. [22] it was also found that the third delocalized state with very unusual energy dependence of the localization length is present at the center of LL. Below we will also attempt to interpret this observation.

II. NONDIAGONAL DISORDER

The way to incorporate the bond disorder into the description of the electron states was proposed by Ando in Ref. [21]. One has to add to the bare 4×4 Hamiltonian of graphene,

$$\hat{H}_0 = v_F \begin{pmatrix} 0 & \pi_x - \pi_y & 0 & 0 \\ \pi_x + \pi_y & 0 & 0 & 0 \\ 0 & 0 & 0 & \pi_x + \pi_y \\ 0 & 0 & \pi_x - \pi_y & 0 \end{pmatrix}, \quad (5)$$

a perturbation

$$\hat{U}_i(\boldsymbol{r}) = \begin{pmatrix} 0 & z_A^* z_B & 0 & z_A^* z_B' \\ z_B^* z_A & 0 & z_B^* z_A' & 0 \\ 0 & z_A'^* z_B & 0 & z_A'^* z_B' \\ z_B'^* z_A & 0 & z_B'^* z_A' & 0 \end{pmatrix} u(\boldsymbol{r} - \boldsymbol{r}_i), \quad (6)$$

where $z_X = e^{i\boldsymbol{K}\cdot\boldsymbol{R}_X}$, $z_X' = e^{i\boldsymbol{K}'\cdot\boldsymbol{R}_X}$ with $X = A, B$, and $u(\boldsymbol{r} - \boldsymbol{r}_i)$ encodes the change of the hopping parameter upon the alternation of the bond i. Then the matrix, describing the bond disorder, takes the form $\sum_i \hat{U}_i$.

Note that [13] the Hamiltonian Eq. (5) represents the continuous limit of the microscopic Hamiltonian Eq. (1), and its matrix form captures only the low-energy states close to the points K and K' in the momentum space. The general form of the four-component eigenvectors of $\hat{H}_0$ is $(\psi_A^K, \psi_B^K, \psi_A^{K'}, \psi_B^{K'})$. In the absence of disorder, the $n = 0$ eigenvector has only one nonzero component corresponding to B sites in the valley K and to A sites in the valley K'. The randomness in the hopping parameter couples B sites in the valley K to the A sites in the valley K'.

The fact that there are three types of bonds in graphene is captured in the perturbation $\hat{U}_0$ by nondiagonal matrix element $z_B^* z_A$, where, with proper choice of axes, $(z_B^* z_A')$ takes three values, namely, 1, $\exp(2\pi i/3)$, and $\exp(-2\pi i/3)$, depending on the position of the bond [21].

Upon introducing the random function

$$h(\boldsymbol{r}) = \sum_{\text{bonds } i} c_i u(\boldsymbol{r} - \boldsymbol{r}_i) + e^{2\pi i/3} \sum_{\text{bonds } j} c_j u(\boldsymbol{r} - \boldsymbol{r}_j) + e^{-2\pi i/3} \sum_{\text{bonds } l} c_l u(\boldsymbol{r} - \boldsymbol{r}_l), \quad (7)$$

where the coefficients c_i, c_j, and c_l take the values 0 or 1 depending on whether or not the corresponding bond is perturbed, we rewrite a system of equations for the components of the spinor in the form

$$\begin{aligned} E\psi_A^K &= v_F(\pi_x - i\pi_y)\psi_B^K + h(\boldsymbol{r})\psi_B^{K'}, \\ E\psi_B^K &= v_F(\pi_x + i\pi_y)\psi_A^K + h(\boldsymbol{r})\psi_A^{K'}, \\ E\psi_A^{K'} &= v_F(\pi_x + i\pi_y)\psi_B^{K'} + h^*(\boldsymbol{r})\psi_B^K, \\ E\psi_B^{K'} &= v_F(\pi_x - i\pi_y)\psi_A^{K'} + h^*(\boldsymbol{r})\psi_A^K. \end{aligned} \quad (8)$$

In this system we have kept only the terms responsible for the intervalley scattering. In the absence of this scattering, the amplitudes ψ_B^K and $\psi_A^{K'}$ correspond to the $\phi_{0,k}(x)$, i.e., to zeroth LL, while the amplitudes ψ_A^K and $\psi_B^{K'}$ are zero. When the disorder strength is much smaller than the distance between the LLs, the system Eq. (8) simplifies to the 2×2 system

$$\begin{aligned} E\psi_B^K &= h(\boldsymbol{r})\psi_A^{K'}, \\ E\psi_A^{K'} &= h^*(\boldsymbol{r})\psi_B^K. \end{aligned} \quad (9)$$

We can write the amplitude $\psi_A^{K'}$ and ψ_B^K as a linear combination of $\phi_{0,k}$,

$$\begin{aligned} \psi_B^K &= \sum_\kappa e^{i\kappa y}\phi_{0,\kappa}(x)B_\kappa^K, \\ \psi_A^{K'} &= \sum_q e^{iqy}\phi_{0,q}(x)A_q^{K'}. \end{aligned} \quad (10)$$

Substituting Eq. (10) into Eq. (9), we get

$$\begin{aligned} EB_\kappa^K &= \sum_q h_{\kappa,q}A_q^{K'}, \\ EA_\kappa^{K'} &= \sum_q h_{\kappa,q}^* B_q^K, \end{aligned} \quad (11)$$

where $h_{\kappa,q}$ is matrix element of $h(\boldsymbol{r})$ between the eigenfunctions, $e^{i\kappa y}\phi_{0,\kappa}(x)$ and $e^{iqy}\phi_{0,q}(x)$, of $n = 0$ LL.

III. DENSITY OF STATES

A. Perturbative approach

From Eq. (10) it becomes apparent that the problem of the broadening of $n = 0$ LL by the bond disorder reduces to the model introduced by Hikami, Shirai, and Wegner, in Ref. [29]. The Hamiltonian of Ref. [29],

$$\hat{H}_{HSW} = \begin{pmatrix} \frac{1}{2m}\left(\mathbf{p} - \frac{e}{c}\boldsymbol{A}\right)^2 & h_1(x,y) + ih_2(x,y) \\ h_1(x,y) - ih_2(x,y) & \frac{1}{2m}\left(\mathbf{p} - \frac{e}{c}\boldsymbol{A}\right)^2 \end{pmatrix}, \quad (12)$$

pertains to parabolic spectrum with effective mass m. The random fields, $h_1(x, y)$ and $h_2(x, y)$, are assumed uncorrelated.

When the states are restricted to zeroth LL, the eigenvectors of the Hamiltonian $\hat{H}_{HSW}$ are the spinors with components

$$\alpha(x,y)=\sum_k A_k e^{iky}\phi_{0,k}(x,y),\ \beta(x,y)=\sum_k B_k e^{iky}\phi_{0,k}(x,y), \tag{13}$$

where A_k and B_k satisfy the system Eq. (10).

In Ref. [29], the Hamiltonian Eq. (12) was introduced to describe the effect of a specific type of disorder on electron states in $n=0$ LL. It was assumed that the bare states were of $N=2$ types, and the disorder scattering was allowed only between the states of different type. Upon examination of the expansion of the diffusion coefficient in powers of disorder, it was concluded that the state, $E=0$, with E measured from $\frac{eB\hbar}{2mc}$, is delocalized. With regard to the density of states, the self-consistent Born approximation [1] for the Hamiltonian Eq. (12) yields a semicircle shape. Taking the large-N limit, the authors concluded that the density of states diverges logarithmically at $E=0$. Later [30], upon employing the semiclassical description, Lee demonstrated that, in addition to $E=0$ delocalized state, the model of Ref. [29] contains two additional delocalized states of the conventional quantum Hall type. Subsequent numerical simulations [31] confirmed the existence of all three delocalized states; see however Ref. [32].

In graphene, the role of states of two types, considered in Ref. [29], is played by the states at K and K' points, while the scattering between them is provided by the bond disorder.

Below we propose an alternative approach to describe the eigenstates of Eq. (12). We start by introducing the new variables

$$a_k=\tfrac{1}{2}(A_k+B_k),\quad b_k=\tfrac{1}{2}(A_k-B_k). \tag{14}$$

With these variables, the system Eq. (11) takes the form

$$Ea_\kappa-\sum_q(h_1)_{\kappa,q}a_q=-i\sum_q(h_2)_{\kappa,q}b_q, \tag{15}$$

$$Eb_\kappa+\sum_q(h_1)_{\kappa,q}b_q=i\sum_q(h_2)_{\kappa,q}a_q. \tag{16}$$

Our main assumption in analyzing the eigenstates of the system Eq. (15) is that the magnitudes and statistical properties of $h_1(x,y)$ and $h_2(x,y)$ fields are completely different. In particular, we assume that the magnitude of $h_2(x,y)$ is much smaller than the magnitude of $h_1(x,y)$ and treat $h_2(x,y)$ *perturbatively*.In zeroth order, the eigenfunctions, $\chi_\nu^+(x,y)$ and $\chi_\mu^-(x,y)$, of the system Eq. (15) are the states of $n=0$ LL in the *potentials* $h_1(x,y)$ and $-h_1(x,y)$, respectively. Upon switching on the field $h_2(x,y)$, the eigenfunctions, $\chi_\nu^+(x,y)$ and $\chi_\mu^-(x,y)$, get coupled. The coupling amplitude is equal to $\int d\boldsymbol{r}(\chi_\nu^+)^*h_2(x,y)(\chi_\mu^-)$. To proceed, we further assume that the correlation length, R_c, of $h_2(x,y)$ is much bigger than ℓ_B. Then $h_2(x,y)$ in the integrand can be treated as a constant. Consequently, the coupling amplitude reduces to the overlap integral of χ_ν^+ and χ_μ^-.

Our prime observation is that this integral is nonzero only when χ_ν^+ and χ_μ^- correspond to energy E in the potential $h_1(x,y)$ and to $-E$ in the potential $-h_1(x,y)$, respectively. Then the functions χ_ν^+ and χ_μ^- are the same. Any other function χ_μ^- in the potential $-h_1(x,y)$ has its counterpart in the potential $h_1(x,y)$, which corresponds to energy different from the state χ_ν^+. Thus, it is orthogonal to χ_ν^+. This situation is illustrated in Fig. 1.

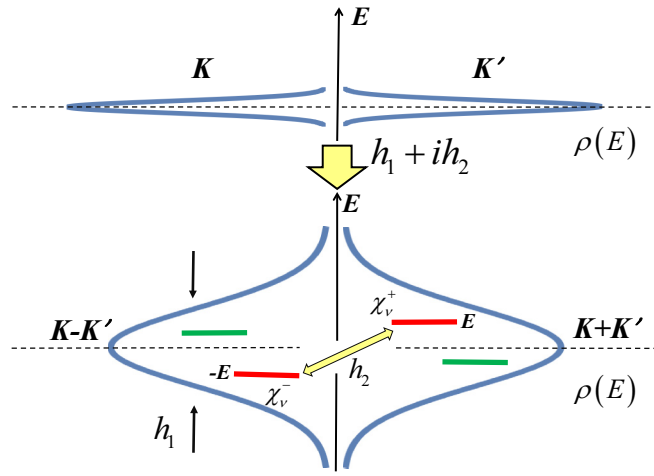

FIG. 1. In order to describe the effect of $K\to K'$ scattering, described by the nondiagonal term h_1+ih_2, on the density of states, we switch to the basis, $K\pm K'$. In the absence of h_2, the field $h_1(x,y)$ broadens the zeroth level, leading to a "Gaussian"-type shape of the density of states. Note that, the wave function χ_ν^+ of the state E in the potential $h_1(x,y)$ is the same as the wave function χ_ν^- of the state $-E$, in the potential $-h_1(x,y)$; see Eqs. (15) and (16). A smooth field, $h_2(x,y)$, couples χ_ν^+ to χ_ν^- (shown with red), but does not couple them to any other states (shown with green). As a result of this coupling, the levels E and $-E$ are repelled away from the center, $E=0$.

We conclude that, upon switching on the random field $h_2(x,y)$, the modified states are determined upon diagonalizing the 2×2 matrix,

$$\begin{pmatrix} E_\nu & i(h_2)_{\nu,\nu} \\ -i(h_2)_{\nu,\nu} & -E_\nu \end{pmatrix}, \tag{17}$$

where E_ν is the bare energy, and the nondiagonal element $(h_2)_{\nu,\nu}$ stands for the coupling amplitude. The modified energies are given by

$$\tilde{E}_\nu=\pm\left[E_\nu^2+|(h_2)_{\nu,\nu}|^2\right]^{1/2}. \tag{18}$$

Overall, the effect of $h_2(x,y)$ amounts to the repulsion of the states E_ν away from the center $E=0$.From the fact that the values E_ν and $(h_2)_{\nu,\nu}$ are statistically independent, we readily arrive at the general expression for the modified density of states,

$$\rho(\tilde{E})=\int dE\,\rho_{h_1}(E)\int dh_2\mathcal{P}(h_2)\,\delta\left[\tilde{E}-\left(E^2+h_2^2\right)^{1/2}\right], \tag{19}$$

where $\rho_{h_1}(E)$ is the average density of states in the potential $h_1(x,y)$. The form of this density of states depends on whether the correlation length of $h_1(x,y)$ is bigger or smaller than the magnetic length. For long-range disorder $\rho_{h_1}(E)$ is Gaussian,

$$\rho_{h_1}(E)=\frac{1}{2\pi^{3/2}\ell_B^2\Gamma}\exp\left(-\frac{E^2}{\Gamma^2}\right), \tag{20}$$

where the width, Γ, is simply $\Gamma_L = \langle h_1(x,y)^2\rangle^{1/2}$, i.e., the r.m.s. value of the potential. In the opposite limit of short-range disorder with a correlator

$$\langle h_1(\boldsymbol{r})h_1(\boldsymbol{r}_1)\rangle = w\delta(\boldsymbol{r}-\boldsymbol{r}_1) \tag{21}$$

the exact density of states found by Wegner in Ref. [3] has the form

$$\rho_{h_1}(E) = \frac{1}{2\pi^2\ell_B^2}\frac{\partial}{\partial E}\{\arctan[G(E/\Gamma)]\},\ G(z) = \int_0^z dt\, e^{t^2}, \tag{22}$$

with $\Gamma = \Gamma_S = (w/2\pi\ell_B^2)^{1/2}$. While Γ_S grows with magnetic field and Γ_L does not, the shape Eq. (22) is close to Gaussian.

Following our assumption that $h_2(x,y)$ is smooth, we choose the Gaussian form for $\mathcal{P}(h_2)$,

$$\mathcal{P}(h_2) = \frac{1}{\pi^{1/2}\gamma}\exp\left(-\frac{h_2^2}{\gamma^2}\right), \tag{23}$$

with $\gamma = \langle h_2(x,y)^2\rangle^{1/2}$.

Upon substituting Eqs. (20) and (23) into the expression Eq. (19) for the density of states, we introduce polar coordinates $E = R\cos\varphi$ and $h_2 = R\sin\varphi$ and cast it in the form

$$\rho(\tilde{E}) = \frac{1}{2\pi^2\ell_B^2\Gamma\gamma}\int_0^\infty dRR\int_0^{2\pi} d\varphi \times \exp\left[-R^2\left(\frac{\cos^2\varphi}{\Gamma^2}+\frac{\sin^2\varphi}{\gamma^2}\right)\right]\delta(\tilde{E}-R). \tag{24}$$

Integration over R is performed using the δ function, and the integral over φ reduces to the modified Bessel function $I_0(z)$. The final result reads

$$\rho(\tilde{E}) = \frac{|\tilde{E}|}{\pi\ell_B^2\Gamma\gamma}\exp\left[-\frac{\tilde{E}^2}{2}\left(\frac{1}{\Gamma^2}+\frac{1}{\gamma^2}\right)\right] \times I_0\left[\frac{\tilde{E}^2}{2}\left(\frac{1}{\Gamma^2}-\frac{1}{\gamma^2}\right)\right]. \tag{25}$$

The fact that $\rho(\tilde{E})$ behaves as $|\tilde{E}|$ at small energies is a natural consequence of the level repulsion. It is also natural that, for symmetric disorder $\Gamma = \gamma$, Eq. (25) reduces to the Wigner-Dyson distribution, as in Ref. [31]. Under the assumption adopted above, that the disorder $h_2(x,y)$ is weak, the shape of the density of states develops a sharp feature at small energies, as illustrated in Fig. 2, which is somewhat reminiscent of the numerical data [20–27], but does not capture the robust low-energy behavior revealed in these papers. We argue that the reason for the discrepancy lies in the fact that we disregarded the energy dependence of the matrix element $(h_2)_{\nu,\nu}$. Namely, when we assumed the correlation length R_c of $h_2(x,y)$ is much bigger than ℓ_B, we overlooked the fact that upon approaching $\tilde{E}=0$ the eigenfunctions χ_ν^+ and χ_ν^- become progressively extended,

$$\langle(h_2)_{\nu,\nu}^2\rangle = \int dr_1|\chi_\nu^+(r_1)|^2dr_1\int dr_2|\chi_\nu^-(r_2)|^2dr_2 \times\langle h_2(r_1)h_2(r_2)\rangle \sim \gamma\left(\frac{R_c}{\mathcal{L}(E)}\right)^2, \tag{26}$$

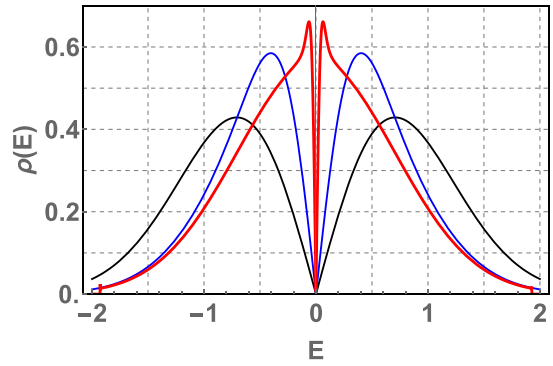

FIG. 2. The shapes of the density of states are plotted from Eq. (25) vs the dimensionless energy E/Γ for three different values of the ratio γ/Γ: 1 (black), 0.4 (blue), 0.05 (red). Black line corresponds to the Wigner-Dyson distribution. For small γ/Γ a fine structure emerges near $E=0$.

where $\mathcal{L}(E)$ is the energy-dependent localization length of the wave functions χ_ν^+ and χ_ν^-. We see that the repulsion of energy levels from the band center, $E=0$, gets strongly suppressed at $E\to 0$. This observation is illustrated in Fig. 3. The area corresponding to the $\mathcal{L}(E)^2$ state E contains $(\frac{\mathcal{L}(E)}{R_c})^2$ squares within which $h_2(\boldsymbol{r})$ is constant. Since the contributions of these squares to $(h_2)_{\nu,\nu}$ are random, the typical value of $(h_2)_{\nu,\nu}$ is suppressed by a factor $\sim(\frac{R_c}{\mathcal{L}(E)})$. This is certainly a hand-waving argument. Strictly speaking, with $h_2(\boldsymbol{r})$ changing in space, the state χ_ν^- gets coupled to *all* the states χ_ν^+. It is, however, important that the contributions to the matrix element from positive and negative energies almost cancel each other at small E.

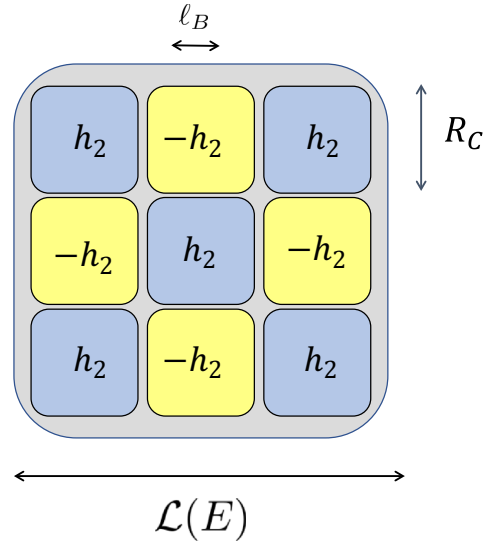

FIG. 3. A cartoon illustrating the suppression of the repulsion of energies E and $-E$ near zero energy. Although the correlation radius R_c is bigger than the magnetic length ℓ_B, the extension $\mathcal{L}(E)$ of the wave functions grows with decreasing E, and, eventually, exceeds R_c. Then the matrix element $(h_2)_{\nu,\nu}$, responsible for repulsion, can be viewed as a sum of $[R_c/\mathcal{L}(E)]^2$ random contributions.

B. Shapes of the density of states

A minimal ansatz to incorporate the suppression of the repulsion of the levels E and $-E$ into the density of states Eq. (19) is to assume that the matrix element $(h_2)_{\nu,\nu}$ still obeys the Gaussian distribution, but the r.m.s. value γ is a function of E.

Due to finite R_c, the state ν corresponding to the energy E will be coupled by $h_2(x,y)$ not only to the state $-E$ but to the states corresponding to different energies. We will still assume that only $(h_2)_{\nu,\nu}$ is nonzero, since the degree of violation of the orthogonality is $\sim \ell_B^2/R_c^2$, which is small. Then, performing integration over h_2 in Eq. (19), we arrive at the following expression for the density of states:

$$\rho(\tilde{E}) = \frac{|\tilde{E}|}{2\pi\ell_B^2\Gamma}\int_0^{\tilde{E}} \frac{dE}{\gamma(E)(\tilde{E}^2-E^2)^{1/2}} \times \exp\left[-\left(\frac{E^2}{\Gamma^2}+\frac{\tilde{E}^2-E^2}{\gamma^2(E)}\right)\right]. \quad (27)$$

Concerning the functional dependence of $\gamma(E)$, we know that it is constant far from $E=0$ and falls off as $R_c/\mathcal{L}(E)$ as $E\to 0$. To analyze the density of states, we chose the following interpolation:

$$\gamma(E) = \gamma_0 \tanh\left[\frac{R_c}{\mathcal{L}(E)}\right] = \gamma_0 \tanh\left[\frac{R_c}{\ell_B}\left(\frac{E}{\Gamma}\right)^{\kappa}\right]. \quad (28)$$

Other forms of $\gamma(E)$ yielded similar results. In fact, Eq. (27) contains three independent parameters, which we varied. The first is the strength γ_0 of the disorder $h_2(x,y)$, as in Eq. (23), the second is the ratio R_c/ℓ_B, which we assume to be big, and, finally, the exponent κ in the energy dependence of the localization length. For the conventional quantum Hall critical point the value of κ is 2.3. In analysis of the shape $\rho(E)$ we have changed one parameter keeping the other two constant. The results are shown in Fig. 4. The main message of Fig. 4 is that, as we vary the parameters, the general shape of $\rho(E)$ remains unchanged.

From Fig. 4(a) we conclude that when the exponent κ increases, the anomaly at $E=0$ becomes more and more pronounced. Comparing to Fig. 2, we see that the behavior of $\rho(E)\propto|E|$ gets modified to a narrow peak. The explanation for this is straightforward: delocalization of states near $E=0$ in the absence of $h_2(x,y)$ results in suppression of their repulsion when $h_2(x,y)$ is switched on. This suppression becomes more effective upon increasing κ. Then the origin of the peak is that, while the states with $E\sim\Gamma$ are shifted by h_2 either to the left or to the right, depending on the sign of E, the low-energy states retain their positions. Obviously, the analysis of the perturbation expansion in terms of h_1 and h_2, of the density of states up to a finite order, cannot capture this effect. This is because the finite-order expansion does not capture the delocalization of the wave functions.

Figure 4(b) suggests that the prime effect of increasing the strength of h_2 is the general broadening of the density of states, while the behavior at small E changes weakly.

Evolution of the curves in Fig. 4(c) can be understood as follows. We assumed that h_2 couples the state χ_ν^+ only to the state χ_ν^-. The bigger the R_c, the more accurate is this assumption. Then, the bigger the R_c, the more pronounced is the separation of the density of states into the central peak and two split maxima.

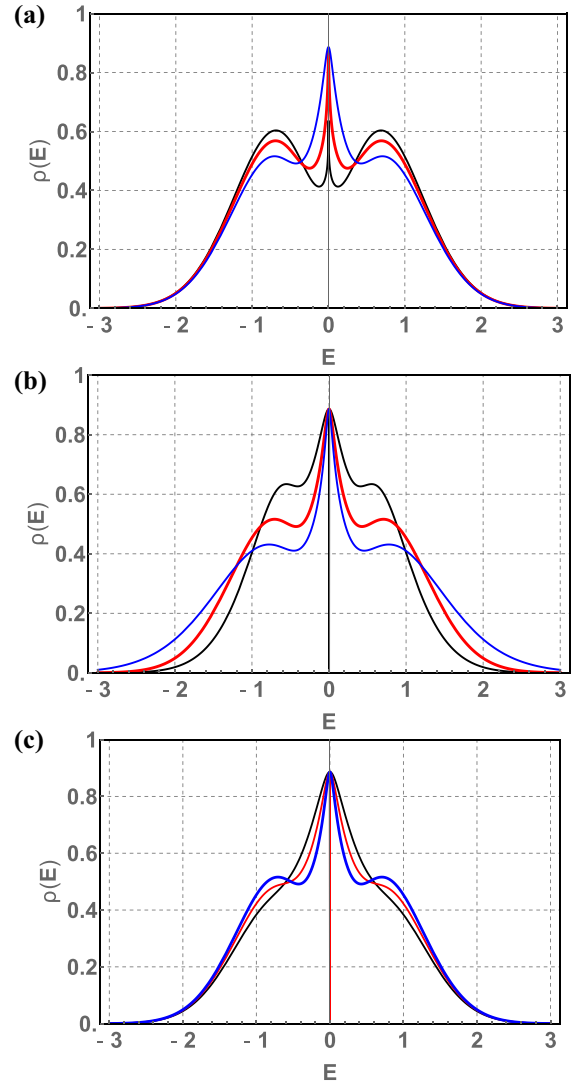

FIG. 4. The density of states is plotted from Eqs. (27) and (28) vs the dimensionless energy, E/Γ, by varying three parameters: κ, γ_0/Γ, R_c/ℓ_B. In the top panel $\rho(E)$ is plotted for three values of κ: 1.2 (black), 1.5 (red), 2 (blue), with $\gamma_0/\Gamma=1$ and $R_c/\ell_B=8$. In the middle panel (b), γ_0/Γ takes values 0.5 (black), 1 (red), 1.5 (blue), while $\kappa=2$ and $R_c/\ell_B=8$. In the bottom panel (c) $\rho(E)$ is for the parameters R_c/ℓ_B: 3 (black), 5 (red), 8 (blue), with γ_0/Γ and κ taking values 1 and 2, respectively.

From all the curves in Fig. 4 the most reminiscent of the numerical simulation results [20–27] is the red curve in Fig. 4(a).

C. White-noise disorder

In this subsection we lift the requirement that the correlation radius R_c of the field $h_2(x,y)$ is much bigger than magnetic length. It was this requirement that ensured the repulsion of the levels E_ν and $-E_\nu$. When $h_2(x,y)$ is short ranged, it couples the $K-K'$ level E_ν to all $K+K'$ levels, E_μ. Still, we will see that coupling of E_ν to $-E_\nu$ remains

distinguished, since the corresponding states have the same wave functions.

For this purpose we search for the solution of the system Eqs. (15) and (16) in the form of expansion,

$$\Psi^{(K+K')} = \sum_{\nu} c_\nu \chi_\nu^+, \quad \Psi^{(K-K')} = \sum_{\mu} d_\mu \chi_\mu^-, \tag{29}$$

where χ_ν^+ and χ_μ^- are the eigenfunctions of the system Eqs. (15) and (16) in the absence of $h_2(x,y)$. For a finite h_2 we arrive at the following system for the coefficients c_ν and d_μ:

$$\begin{aligned} &c_\nu(E_\nu^+ - E)\chi_\nu^+ + \sum_{\nu'\neq\nu} c_{\nu'}(E_{\nu'}^+ - E)\chi_{\nu'}^+ \\ &= -ih_2(x,y)\left[d_\mu \chi_\mu^- + \sum_{\mu'\neq\mu} d_{\mu'}\chi_{\mu'}^-\right], \\ &d_\mu(E_\mu^- - E)\chi_\mu^+ + \sum_{\mu'\neq\mu} d_{\mu'}(E_{\mu'}^- - E)\chi_{\mu'}^- \\ &= ih_2(x,y)\left[c_\nu \chi_\nu^+ + \sum_{\nu'\neq\nu} c_{\nu'}\chi_{\nu'}^+\right]. \end{aligned} \tag{30}$$

For a given ν, we treat c_ν and d_ν as zero-order terms, and express c_μ and d_μ with $\mu \neq \nu$ through them. Substituting c_μ, d_μ back into the system, we get

$$\left[E_\nu^+ - E - \frac{|(h_2)_{\nu,\nu}|^2}{E_\nu^- - E}\right]c_\nu = d_\nu S_\nu, \tag{31}$$

$$\left[E_\nu^- - E - \frac{|(h_2)_{\nu,\nu}|^2}{E_\nu^+ - E}\right]d_\nu = -c_\nu S_\nu, \tag{32}$$

where S_ν stands for the sum

$$S_\nu = \sum_{\mu\neq\nu} \frac{|(h_2)_{\nu,\mu}|^2}{E_\mu^- - E} = \sum_{\nu\neq\mu} \frac{|(h_2)_{\nu,\mu}|^2}{E_\mu^+ - E}. \tag{33}$$

Multiplying Eqs. (31) and (32), we get the following equation for E:

$$\left[\left(E^2 - E_\nu^2\right) - |(h_2)_{\nu,\nu}|^2\right]^2 = \left(E^2 - E_\nu^2\right){S_\nu}^2, \tag{34}$$

the solution of which reads

$$E^2 = E_\nu^2 + \left[\left(|(h_2)_{\nu,\nu}|^2 + \frac{{S_\nu}^2}{4}\right)^{1/2} \pm \frac{S_\nu}{2}\right]^2. \tag{35}$$

This equation is a generalization of Eq. (18).

We can now estimate the accuracy of keeping only the diagonal elements of $h_2(x,y)$. If the energy E_ν is in the "body" of the band broadened by the potential $h_1(x,y)$, then only the neighboring states contribute to S. This is because the overlap with states at distance $x \gg \ell_B$ is small as $\exp(-x^2/2\ell_B^2)$. For a neighboring state, the typical value of the denominator of Eq. (33) is $\sim \Gamma$, while the numerator is $\sim \gamma_0^2$. Thus, the relative correction to $(h_2)_{\nu,\nu}^2$ is $\sim \gamma_0^2/\Gamma^2$, i.e., it is small.

The estimate for the correction S_ν in the case where $E_\nu \ll \Gamma$ should be carried out differently. With $h_2(x,y)$ being the white noise, the average $\langle S_\nu \rangle$ contains the combination

$$\sum_{\mu} \frac{|\chi_\nu^+(\boldsymbol{r})|^2 |\chi_\mu^-(\boldsymbol{r})|^2}{E_\nu^+ - E_\mu^-}, \tag{36}$$

which depends on the correlation between functions χ_ν^+ and χ_μ^-, which are the eigenfunctions in *different* potentials, $h_1(x,y)$ and $-h_1(x,y)$.

It is known, see, e.g., Refs. [33–35], that the correlation of the critical eigenfunctions in the *same* potential is quantified as

$$\int d\boldsymbol{r}\, |\chi_\nu^+(\boldsymbol{r})|^2 |\chi_{\nu'}^+(\boldsymbol{r})|^2 \delta(E_\nu^+ - E_{\nu'}^+) \propto |\frac{\Gamma}{E_\nu^+ - E_{\nu'}^+}|^{\eta/2}, \tag{37}$$

where η is the exponent characterizing the fractal structure of critical eigenfunctions. Recall now that the wave functions χ_ν^+ and χ_μ^- are the same when they correspond to opposite energies, $E_\nu^+ = -E_\mu^-$. Then we can use Eq. (37) to estimate $\langle S_\nu \rangle$,

$$\int \frac{dE_\mu^-\, \rho_{h_1}(E_\mu^-)}{E_\nu^+ - E_\mu^-} \left|\frac{\Gamma}{E_\nu^+ + E_\mu^-}\right|^{\eta/2} \propto \frac{1}{|E_\nu^+|^{\eta/2}}. \tag{38}$$

The above equation suggests that $\langle S_\nu \rangle$ increases upon approaching $E_\nu^+ \to 0$. Still, it loses to the diagonal term, $(h_2)_{\nu,\nu}$. This is because a typical $(h_2)_{\nu,\nu}$ is proportional to $1/\mathcal{L}(E)$, see Eq. (26), while ${S_\nu}^2$ is proportional to $1/\mathcal{L}^2(E)$.

IV. DELOCALIZED STATES

The only physically transparent description of the quantum Hall transition is the Chalker-Coddington (CC) network model of Ref. [36], which is a quantum generalization of the classical percolation. To apply this model in our case, one should assume that both fields $h_1(x,y)$ and $h_2(x,y)$ are smooth. Then the semiclassical energies [30] are determined by local values of h_1 and h_2 and are equal to $\mathcal{E}_\pm = \pm(h_1^2 + h_2^2)^{1/2}$. Within the prefactor, the distribution function $\mathcal{F}(\mathcal{E}_+)$ of $\mathcal{E}_+$ is given by Eq. (25). Then the percolation threshold, $E = E_c$, is found from the condition $\int_0^{E_c} d\mathcal{E}_+\, \mathcal{F}(\mathcal{E}_+) = \frac{1}{2}$. If h_1 and h_2 are statistically equivalent, then $\mathcal{F}(\mathcal{E}_+) = \frac{2\mathcal{E}_+}{\Gamma^2}\exp(-\frac{\mathcal{E}_+^2}{\Gamma^2})$. This yields $E_c = 0.7\Gamma$, i.e., the delocalized state lies slightly above the maximum, 0.5Γ, of the density of states. This is consistent with the numerical result of Ref. [31], although the simulations were performed for the short-range disorder.

Classical percolation at $E = \pm E_c$ transforms into the conventional quantum Hall transitions when the tunneling through the saddle points, defined by the conditions $\frac{\partial}{\partial x}(h_1^2 + h_2^2) = 0$ and $\frac{\partial}{\partial y}(h_1^2 + h_2^2) = 0$ (and opposite signs of the second derivatives), are taken into account.

There is no classical picture underlying the delocalized state at $E = 0$, revealed in Ref. [29]. A peculiar feature of this delocalization established numerically in Refs. [22,31], see also Ref. [37], is that the critical exponent is anomalously small, $\nu \approx 0.3$. It is even smaller than the $\nu = \frac{4}{3}$ for classical percolation and for the random flux model [38–42]. It is likely that the accuracy of simulations in Refs. [20,22,31] was limited by the size effects.

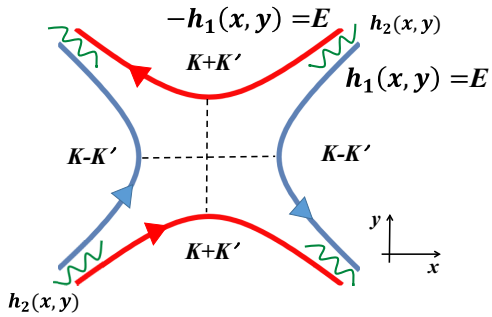

FIG. 5. Blue equipotentials are $h_1(x,y)=E$, while red equipotentials are $-h(x,y)=E$. Red and blue equipotentials are coupled via the random field $h_2(x,y)$. Instead of tunneling through the saddle point, $\frac{\partial h_1}{\partial x}=0$, $\frac{\partial h_1}{\partial y}=0$, the transports proceeds as blue → red → blue and red → blue → red. In this way, the saddle point gets bypassed. The resulting energy dependence of the localization length originating from the dependence of the transmission through the saddle point is weak.

A small critical exponent suggests that the localization length depends weakly on energy near $E=0$. Below we invoke the CC model to explain a possible origin of this weak dependence. The explanation is based on Fig. 5. Within the CC model, the behavior of the localization length on energy E is governed by tunneling via the saddle points separating two equipotentials; see Fig. 5. Equipotentials, $h_1(x,y)=0$, form a percolation network. Consider two blue equipotentials corresponding to $K-K'$ states. Note that, for the states corresponding to $K+K'$, the random potential is equal to $-h_1(x,y)$. Thus, the equipotentials shown in Fig. 5 in red are rotated by 90°. Equipotentials $h_1(x,y)=E$ and $-h_1(x,y)=E$ are coupled by the random field $h_2(x,y)$. This suggests that energy-dependent tunneling via the saddle point does not affect the structure of the low-energy states. The reason for this is that the saddle point is *bypassed* [43] by the alternative channels: blue → red → blue and red → blue → red; see Fig. 5. Such a bypassing results in a weak energy dependence of the transmission of the saddle points and, thus, in a weak energy dependence of the localization length until E becomes anomalously small. On the other hand, smallness of the critical exponent manifests itself in a similar way. Namely, with localization length behaving as $E^{-\nu}$, for small ν, this length remains almost constant as E approaches zero, and "shoots up" only in a very narrow vicinity of $E=0$. In this way, the cartoon Fig. 5 yields a qualitative explanation of the smallness of ν established numerically.

V. DISCUSSION AND CONCLUDING REMARKS

(i) By assuming that the bond disorder in one direction is much stronger than in the other two, which is equivalent to the condition $h_2(x,y)\ll h_1(x,y)$, we arrived at the following scenario for the shape of the density of states of the $n=0$ LL: the field $h_1(x,y)$ broadens the level into a band, while the field $h_2(x,y)$ is responsible for the repulsion of the levels *from the center of the band* facilitated by $K\to K'$ scattering. The states with $E>0$ are shifted up, while the states with $E<0$ are shifted down. Most importantly, the low-energy states remain unshifted, which leads to the three-peak structure of the disorder-broadened band.

(ii) Certainly, the assumption $h_2(x,y)\ll h_1(x,y)$ is artificial and does not correspond to the simulations of Refs. [20–27]. However, treatment of $h_1(x,y)$ and $h_2(x,y)$ on equal footing is possible only within the self-consistent Born approximation, leading to the semicircle shape [29] with a width $\sqrt{2}\Gamma$. This means that the diagrams taken into account within the self-consistent Born approximation [1] do not capture properly the repulsion of the states away from the band center, $E=0$. The picture of Ref. [30] also does not allow us to make quantitative predictions about the shape of the density of states near $E=0$.

The model of Ref. [29] is unique, in the sense that delocalization of states has a dramatic back effect on the density of states; self-consistent Born approximation is not sensitive to the localization. Also, evaluating any particular diagram in the perturbation expansion of the density of states will not reveal an energy scale smaller than Γ. We inferred such a small scale from delocalization of $K-K'$ and $K+K'$ eigenstates in the potential, $h_1(x,y)$, assuming that $h_2(x,y)$ is absent. Note that, in the simulations of Refs. [25,26], the central peak in the density of states was hardly pronounced. Accordingly, the authors did not find any evidence for delocalization at $E=0$.

The specifics of the Hamiltonian Eq. (12) with regard to the behavior of the eigenstates at low energies were discussed in Ref. [31]. It was pointed out that these specifics originate from the reflection symmetry of the Hamiltonian, $\sigma_z\hat{H}_{HSW}\sigma_z=-\hat{H}_{HSW}$. Interestingly, the numerical simulations of a different model [44], a 1D hopping chain with off-diagonal disorder, described by a Hamiltonian possessing the reflection symmetry, also revealed a three-peak structure of the density of states.

(iii) We have treated the field $h_2(x,y)$ perturbatively. This implies the assumption that the perturbation theory applies even at low energies, so that $h_2(x,y)$ does not modify the structure of the wave functions of the low-energy states. On the other hand, the argument, illustrated in Fig. 5, suggests that the order in which h_2 and E go to zero is important. This can be also seen from the analysis of the expression Eq. (19) for the density of states. In the limit of low energies, the integral in Eq. (19) reduces to

$$\rho(\tilde{E})\propto\int_0^\infty\frac{dz}{z^\kappa}\,\delta\!\left(\frac{E}{E_c}-(z^2+z^{2\kappa})^{1/2}\right),\tag{39}$$

where

$$E_c=\left(\frac{\Gamma^\kappa\ell_B}{\gamma_0 R_c}\right)^{1/(1-\kappa)}.\tag{40}$$

Since γ_0 reflects the magnitude of h_2, it is seen that the result depends on the order of taking the limits $h_2\to 0$ and $E\to 0$.

(iv) Naturally, in the opposite limit, $h_1(x,y)\ll h_2(x,y)$, we will arrive at the same result for the density of states and delocalization. In this limit, one should introduce the variables $A_k\pm iB_k$, instead of the variables $A_k\pm B_k$, Eq. (14). Then $h_2(x,y)$ will be responsible for the broadening of the level, while $h_1(x,y)$ will lead to the repulsion of the states away from $E=0$.

(v) Let as relate the fields $h_1(x, y)$ and $h_2(x, y)$ to the bond disorder in graphene: From Eq. (7) we have

$$h_1(\boldsymbol{r}) = \sum_{\text{bonds}i} c_i u(\boldsymbol{r}-\boldsymbol{r}_i) - \frac{1}{2}\left[\sum_{\text{bonds}j} c_j u(\boldsymbol{r}-\boldsymbol{r}_j) + \sum_{\text{bonds}l} c_l u(\boldsymbol{r}-\boldsymbol{r}_l)\right],$$
$$h_2(\boldsymbol{r}) = \frac{\sqrt{3}}{2}\left[\sum_{\text{bonds}j} c_j u(\boldsymbol{r}-\boldsymbol{r}_j) - \sum_{\text{bonds}l} c_l u(\boldsymbol{r}-\boldsymbol{r}_l)\right]. \quad (41)$$

Our analysis rests on the assumptions that h_1 is much bigger than h_2. Microscopically this means that the concentration of the perturbed i bonds is much bigger than the concentration of the perturbed j and l bonds. In principle this situation can be realized in numerical simulations.

(vi) It is instructive to compare our results with Refs. [20,29] where the attempts were made to calculate the shape of the density of states analytically. In both papers a weak divergence of $\rho(E)$ at $E \to 0$ was found: $\rho(E) \propto \ln^2 E$ in Ref. [29] and $\rho(E) \propto \ln|E|$ in Ref. [20]. Although the analytical approaches in the above papers are different, they both miss an important point, namely that the behavior of $\rho(E)$ and delocalization at the band center are *interconnected*. This follows from our treatment which in the limiting case $h_2 \ll h_1$ becomes exact. It shows that delocalization at $E \to 0$ is responsible for the fact that the $E \to 0$ levels in the random field $h_1(x, y)$ are not shifted by $h_2(x, y)$. Neither large-N expansion in Ref. [29] nor the supersymmetry approach in Ref. [20] are capable of capturing this physics.

ACKNOWLEDGMENTS

We are grateful to T. V. Shahbazyan for illuminating comments. This work was supported by the Department of Energy, Office of Basic Energy Sciences, Grant No. DE-FG02-06ER46313.

[1] T. Ando and Y. Uemura, Theory of quantum transport in a two-dimensional electron system under magnetic fields. I. Characteristics of Level Broadening and Transport under Strong Fields, J. Phys. Soc. Jpn. **36**, 959 (1974).
[2] É. M. Baskin, L. N. Magarill, and M. V. Éntin, Two-dimensional electron-impurity system in a strong magnetic field, Zh. Eksp. Teor. Fiz. **75**, 723 (1978) [Sov. Phys. JETP **48**, 365 (1978)].
[3] F. Wegner, Exact density of states for lowest Landau level in white noise potential superfield representation for interacting systems, Z. Phys. B **51**, 279 (1983).
[4] E. Brézin, D. Gross, and C. Itzykson, Density of states in the presence of a strong magnetic field and random impurities, Nucl. Phys. B **235**, 24 (1984).
[5] L. B. Ioffe and A. I. Larkin, Fluctuation levels and cyclotron resonance in a random potential, Zh. Eksp. Teor. Fiz. **81**, 1048 (1981) [Sov. Phys. JETP **54**, 556 (1981)].
[6] I. Affleck, Two-dimensional disorder in the presence of a uniform magnetic field, J. Phys. C **16**, 5839 (1983).
[7] I. Affleck, Density of states in a uniform magnetic field and a white noise potential, J. Phys. C **17**, 2323 (1984).
[8] W. Apel, Asymptotic density of states for a disordered 2D electron system in a strong magnetic field, J. Phys. C **20**, L577 (1987).
[9] K. A. Benedict and J. T. Chalker, Properties of the disordered two-dimensional electron gas in a strong magnetic field, J. Phys. C **18**, 3981 (1985).
[10] K. A. Benedict and J. T. Chalker, An exactly solvable model of the disordered two-dimensional electron gas in a strong magnetic field, J. Phys. C **19**, 3587 (1986).
[11] K. A. Benedict, The fate of the Lifshitz tails of high Landau levels, Nucl. Phys. B **280**, 549 (1987).
[12] M. E. Raikh and T. V. Shahbazyan, High Landau levels in a smooth random potential for two-dimensional electrons, Phys. Rev. B **47**, 1522 (1993).
[13] Y. Zheng and T. Ando, Hall conductivity of a two-dimensional graphite system, Phys. Rev. B. **65**, 245420 (2002).
[14] M. O. Goerbig, Electronic properties of graphene in a strong magnetic field, Rev. Mod. Phys. **83**, 1193 (2011).
[15] Z. Jiang, Y. Zhang, H. L. Stormer, and P. Kim, Quantum Hall States Near the Charge-Neutrality Dirac Point in Graphene, Phys. Rev. Lett. **99**, 106802 (2007).
[16] L. A. Ponomarenko, R. Yang, R. V. Gorbachev, P. Blake, A. S. Mayorov, K. S. Novoselov, M. I. Katsnelson, and A. K. Geim, Density of States and Zero Landau Level Probed through Capacitance of Graphene, Phys. Rev. Lett. **105**, 136801 (2010).
[17] K. Takase, H. Hibino, and K. Muraki, Probing the extended-state width of disorder-broadened Landau levels in epitaxial graphene, Phys. Rev. B **92**, 125407 (2015).
[18] P. M. Ostrovsky, I. V. Gornyi, and A. D. Mirlin, Theory of anomalous quantum Hall effects in graphene, Phys. Rev. B **77**, 195430 (2008).
[19] W. Zhu, Q. W. Shi, X. R. Wang, J. Chen, J. L. Yang, and J. G. Hou, Shape of Disorder-Broadened Landau Subbands in Graphene, Phys. Rev. Lett. **102**, 056803 (2009).
[20] P. Goswami, X. Jia, and S. Chakravarty, Quantum Hall plateau transition in the lowest Landau level of disordered graphene, Phys. Rev. B **76**, 205408 (2007).
[21] M. Koshino and T. Ando, Splitting of the quantum Hall transition in disordered graphenes, Phys. Rev. B **75**, 033412 (2007).
[22] P. Markoš and L. Schweitzer, Critical conductance of two-dimensional chiral systems with random magnetic flux, Phys. Rev. B **76**, 115318 (2007).
[23] L. Schweitzer, Narrow depression in the density of states at the Dirac point in disordered graphene, Phys. Rev. B **80**, 245430 (2009).
[24] T. Kawarabayashi, Y. Hatsugai, and H. Aoki, Quantum Hall Plateau Transition in Graphene with Spatially Correlated Random Hopping, Phys. Rev. Lett. **103**, 156804 (2009).

[25] A. L. C. Pereira, Splitting of critical energies in the $n = 0$ Landau level of graphene, New J. Phys. **11**, 095019 (2009).

[26] A. L. C. Pereira, C. H. Lewenkopf, and E. R. Mucciolo, Correlated random hopping disorder in graphene at high magnetic fields: Landau level broadening and localization properties, Phys. Rev. B **84**, 165406 (2011).

[27] N. Leconte, F. Ortmann, A. Cresti, and S. Roche, Unconventional features in the quantum Hall regime of disordered graphene: Percolating impurity states and Hall conductance quantization, Phys. Rev. B **93**, 115404 (2016).

[28] Y. Aharonov and A. Casher, Ground state of a spin-1/2 charged particle in a two-dimensional magnetic field, Phys. Rev. A **19**, 2461 (1979).

[29] S. Hikami, M. Shirai, and F. Wegner, Anderson localization in the lowest Landau level for a two-subband model, Nucl. Phys. B **408**, 415 (1993).

[30] D. K. K. Lee, Degenerate Landau bands with interband disorder: A semiclassical picture, Phys. Rev. B **50**, 7743 (1994).

[31] K. Minakuchi and S. Hikami, Numerical study of localization in the two-state Landau level, Phys. Rev. B **53**, 10898 (1996).

[32] C. B. Hanna, D. P. Arovas, K. Mullen, and S. M. Girvin, Effect of spin degeneracy on scaling in the quantum Hall regime, Phys. Rev. B **52**, 5221 (1995).

[33] J. T. Chalker and G. J. Daniell, Scaling, Diffusion, and the Integer Quantized Hall Effect, Phys. Rev. Lett. **61**, 593 (1988).

[34] M. V. Feigel'man, L. B. Ioffe, V. E. Kravtsov, and E. A. Yuzbashyan, Eigenfunction Fractality and Pseudogap State near the Superconductor-Insulator Transition, Phys. Rev. Lett. **98**, 027001 (2007).

[35] V. E. Kravtsov, A. Ossipov, O. M. Yevtushenko, and E. Cuevas, Dynamical scaling for critical states: Validity of Chalker's ansatz for strong fractality, Phys. Rev. B **82**, 161102(R) (2010).

[36] J. T. Chalker and P. D. Coddington, Percolation, quantum tunneling, and the integer quantum Hall effect, J. Phys. C **21**, 2665 (1988).

[37] X. Jia, P. Goswami, and S. Chakravarty, Dissipation and Criticality in the Lowest Landau Level of Graphene, Phys. Rev. Lett. **101**, 036805 (2008).

[38] A. Furusaki, Anderson Localization due to a Random Magnetic Field in Two Dimensions, Phys. Rev. Lett. **82**, 604 (1999).

[39] V. Kagalovsky, B. Horovitz, Y. Avishai, and J. T. Chalker, Quantum Hall Plateau Transitions in Disordered Superconductors, Phys. Rev. Lett. **82**, 3516 (1999).

[40] I. A. Gruzberg, A. W. W. Ludwig, and N. Read, Exact Exponents for the Spin Quantum Hall Transition, Phys. Rev. Lett. **82**, 4524 (1999).

[41] C. Mudry, P. W. Brouwer, and A. Furusaki, Random magnetic flux problem in a quantum wire, Phys. Rev. B **59**, 13221 (1999).

[42] L. Schweitzer and P. Markoš, Scaling at chiral quantum critical points in two dimensions, Phys. Rev. B **85**, 195424 (2012).

[43] D. G. Polyakov and M. E. Raikh, Quantum Hall Effect in Spin-Degenerate Landau Levels: Spin-Orbit Enhancement of the Conductivity, Phys. Rev. Lett. **75**, 1368 (1995).

[44] S. Hikami and A. Zee, Complex random matrix models with possible applications to spin-impurity scattering in quantum Hall fluids, Nucl. Phys. B **446**, 337 (1995).